



Relationship Between Cardiac Fibroblast Activation Protein Activity by Positron Emission Tomography and Cardiovascular Disease

See Editorial by Thackeray

BACKGROUND: FAP (fibroblast activation protein) plays an important role in cardiac wound healing and remodeling. Although initially developed as a theranostic ligand for metastasized cancer, FAPI (FAP inhibitor) tracers have recently been used to study cardiac remodeling following myocardial infarction in small-animal models. The aim of the study was to evaluate the activity of FAP via FAPI–positron emission tomography–computed tomography scans in human hearts.

METHODS: FAPI–positron emission tomography–computed tomography scans of 229 patients of 2 consecutive cohorts (modeling cohort: n=185; confirmatory cohort: n=44) suffering from metastasized cancer were analyzed applying the American Heart Association 17-segment model of the left ventricle. Logistic regression models were created using data from the modeling cohort. Multivariate regression models were established using Akaike information criterion in a step-down approach.

RESULTS: Fourteen percent of patients had preexisting coronary artery disease (n=31), 33% arterial hypertension (n=75), and 12% diabetes mellitus type II (n=28). Forty-three percent had been treated with platinum derivatives (n=100), 14% with anthracyclines (n=32), and 10% had a history of prior radiation to the chest (n=23). High left ventricular FAPI signals correlated with the presence of cardiovascular risk factors (odds ratio [OR], 4.3, $P=0.0029$), a focal myocardial signal pattern (OR, 3.9, $P=0.0068$), diabetes mellitus type II (OR, 4.1, $P=0.046$), and beta-blocker use (OR, 3.8, $P=0.049$) in univariate regression models. In a multivariate analysis, increased signal intensity was significantly higher in patients with cardiovascular risk factors (overweight [OR, 2.6, $P=0.023$], diabetes mellitus type II [OR, 2.9, $P=0.041$], certain chemotherapies [platinum derivatives; OR, 3.0, $P=0.034$], and a history of radiation to the chest [OR, 3.5, $P=0.024$]). A focal enrichment pattern was more frequently observed in patients with known cardiovascular risk factors ($P<0.0001$).

CONCLUSIONS: FAPI–positron emission tomography–computed tomography scans represent a new imaging modality to investigate cardiac FAP. High signal intensities correlate with cardiovascular risk factors and metabolic disease.

Markus B. Heckmann, MD

Finn Reinhardt

Daniel Finke, MD

Hugo A. Katus, MD

Uwe Haberkorn, MD

Florian Leuschner, MD

Lorenz H. Lehmann¹, MD

Key Words: diabetes mellitus
■ fibroblast ■ myocardial infarction
■ risk factors ■ tomography

© 2020 The Authors. *Circulation: Cardiovascular Imaging* is published on behalf of the American Heart Association, Inc., by Wolters Kluwer Health, Inc. This is an open access article under the terms of the [Creative Commons Attribution Non-Commercial-NoDerivs](https://creativecommons.org/licenses/by-nc-nd/4.0/) License, which permits use, distribution, and reproduction in any medium, provided that the original work is properly cited, the use is noncommercial, and no modifications or adaptations are made.

<https://www.ahajournals.org/journal/circimaging>

CLINICAL PERSPECTIVE

Analyzing cardiac FAPI (fibroblast activation protein inhibitor) signal intensity and patterns may be considered in patients receiving FAPI–positron emission tomography–computed tomography scans for cancer staging and progression. Patients with an increased cardiac FAPI signal or focal enrichment patterns may potentially benefit from additional cardiological examinations to diagnose undetected cardiovascular diseases or cardiotoxic side effects to improve cardio-oncological care. Prospective clinical studies are needed to further evaluate the potential use of FAPI–positron emission tomography–computed tomography scans for cardiac risk stratification in ischemic heart disease and myocarditis.

Although the assessment tool box of left ventricular systolic function and the coronary arteries is ever-increasing, cardiac remodeling still lacks a reliable imaging modality.¹

Aside from the profound molecular changes seen in cardiomyocytes, fibroblasts play a key role in cardiac tissue remodeling and wound healing.^{2,3} One characteristic of activated cardiac fibroblasts is the expression of FAP (fibroblast activation protein). In resting fibroblasts, FAP expression is very low and shows a steep increase after myocardial infarction followed by a steady decline over time.^{4,5} The ablation of FAP-positive cells in mice subjected to angiotensin II and phenylephrine reduced cardiac fibrosis and restored systolic function.⁶ These preclinical studies suggest an important role of FAP in cardiac ischemia and pathological remodeling.

In 2018, Lindner et al developed a tracer for positron emission scans that targets FAP. The tracer consists of a quinolone-based FAPI (FAP inhibitor) labeled with a radio nucleoid, which reliably binds and stains FAP.^{7–9} It can be used to measure relative FAP density indicative of activated fibroblasts in different cancer entities. To date, there are no data available that analyze FAPI signal accumulation in human hearts in larger patient cohorts. It remains unclear if increased cardiac FAPI signals are associated with certain cardiovascular risk factors or disease.

The aim of our analysis was to evaluate cardiac tracer accumulation and the role of FAPI–positron emission tomography (PET)–computed tomography (CT) scans in cardiovascular disease in patients with cancer undergoing different cancer therapies.

METHODS

Data Availability

The raw data used in this study are available from the corresponding author on reasonable request.

Study Population and Data Collection

We retrospectively analyzed FAPI-PET-CT scans from adult patients presenting in our nuclear medicine department between 2017 and 2019 with various cancer entities. The study was conducted according to the principles of the Declaration of Helsinki. Approval for this research was granted by the local research ethics committee (S-286/2017). Patient-related information was pseudonymized upon data extraction.

FAPI-PET-CT Scans

FAPI-PET-CT (Siemens Biograph, Siemens Healthcare Diagnostics, Eschborn, Germany) scans were performed according to standard protocol.⁸ One hundred twenty-two to 336 MBq of Ga-68 labeled FAPI were administered intravenously. All patients were scanned 60 minutes after administration. In addition, a subgroup of patients was scanned 10 minutes and 180 minutes after FAPI administration. A low dose whole-body CT scan (130 keV, 30 mAs, CareDose; reconstructed with a soft-tissue kernel to a slice-thickness of 5 mm) was used for attenuation correction and image fusion. A 3-dimensional emission scan (matrix 200×200) was performed, subsequently using FlowMotion (Siemens). The emission data were corrected for randoms, scatter, and decay. Reconstruction was performed with an ordered subset expectation maximization algorithm with 2 iterations/21 subsets and Gauss-filtered to a transaxial resolution of 5 mm at full-width at half-maximum and analyzed using regions of interest measuring standardized uptake values (SUV). Signals were measured in the free left ventricular wall, the blood pool, the aorta, the gluteus muscle, the liver, the lung, and the brain. The mean SUV of the regions of interest was reported. The regions of interest were selected in an area of homogenous signal intensity based on the anatomic structures depicted in the CT scan.

In addition to measuring the free lateral wall in an area without focal signal enrichment, all 17 segments were measured based on the anatomic structure regardless of focal signal enrichment. Segments were attributed to their presumptive corresponding coronary vessel according to the imaging criteria of the American Heart Association.^{10,11} Septal segments were segments 2, 3, 8, 9, and 14. Lateral segments were 5, 6, 11, 12, and 16. Graphs were built in R version 3.6.2 with inhouse scripting using the shape and RColorBrewer packages.^{12–14}

Fluorine-18 fluorodeoxyglucose-PET-CT Scans

All FDG (fluorine-18 fluorodeoxyglucose) -PET-CT scans performed within 12 months of the FAPI-PET-CT scan were also analyzed. FDG-PET-CT scans were performed as previously described.¹⁵ Measurements were performed as in FAPI-PET-CT scans. SUVs and SUV ratios of different organs were compared between FDG and FAPI using a Kruskal-Wallis test. The Spearman method was used to analyze the correlation between FDG and FAPI SUVs.

Patient Characteristics

Patient characteristics included age, sex, cancer entity, body mass index, glomerular filtration rate calculated using the chronic kidney disease epidemiology collaboration formula,

thyroid-stimulating hormone (TSH), cardiovascular risk factors, diabetes mellitus, arterial hypertension, known coronary artery disease, known atrial fibrillation, previous radiation to the chest, chemotherapy (anthracyclines, platinum derivatives, alkylating agents, antimetabolites, taxanes, topoisomerase inhibitors), checkpoint inhibitor use, FAPI signal pattern and cardiac medication (statins, aspirin, ACE [angiotensin-converting enzyme] inhibitor or angiotensin-receptor-blocker and beta-blocker use). For multivariate analyses, patients were divided into 2 cohorts: an initial cohort comprising 80% of patients and a confirmatory cohort comprising 20% of patients. Patients were assigned consecutively to each cohort. Whenever available, echocardiographic findings were also reported.

FAPI-PET-CT scans from representative patients were selected using the k-nearest neighbor algorithm. Applicable patients with the smallest distance to the median were chosen.

Statistical Analysis

Statistical analyses were performed using R version 3.6.2 with the help of the MASS and ggplot2 packages.^{12,16,17} Unless stated otherwise, Non-normal distributed values are reported as median±interquartile range (IQR) and were compared using Wilcoxon rank-sum tests. Normal distributed values are reported as mean±SD. An ANOVA test was performed to test for differences within the groups. Tukey honest significant difference method was applied for *P*-level adjustment.

As SUVs did not follow a standard distribution, SUVs were compared with a pairwise Wilcoxon rank-sum test using Holm method for *P* value adjustment. When available, repetitive measurements were displayed for each patient. When necessary (eg, for linear and logistic regression models), SUVs were logarithmized to achieve normal distribution. Univariate logistic regression models were established using a signal intensity cutoff of 1.3, which was determined by calculating the mean signal intensity and adding ½ of its SD. Odds ratios (ORs) and 95% CIs were calculated. *P*-level adjustment was carried out using the Holm-Bonferroni method. Multivariate models were created selecting the variables according to Akaike information criterion in a step-down approach.^{15,18} Logistic regression results were reported with OR and a 95% CI. A Hosmer-Lemeshow goodness of fit test was performed for each model.

A multivariate linear regression model was established for signal intensity using all variables significantly tested in the multivariate logistic approach. Standardized residuals were calculated with the dataset used to create the model. Outliers were defined as patients with high signal intensities not accurately predicted by our models with calculated residuals above the 95th percentile. The predictive model based on our modeling cohort was subsequently applied to the confirmatory cohort to test for reproducibility.

Outliers were further analyzed by a permutation test comparing patient characteristics of the outlier cohort to 100 000 randomly selected cohorts of the same dataset. The number of times a characteristic occurred as frequently or more frequently in the randomly selected cohorts divided by the number of permutations was used as a *P* value. A *P* value below 0.05 was considered significant. The model was applied to the confirmatory cohort. Standardized residuals were calculated. Outliers were identified using the same cutoff value as in the modeling cohort.

RESULTS

Between 2017 and April 2019 a total of 185 consecutive patients with >20 different metastasized solid tumor entities were recruited and analyzed. Pancreatic carcinoma (n=42), bronchial carcinoma (n=20), colorectal carcinoma (n=14), oropharyngeal cancer (n=13), prostate cancer (n=11), esophageal and gastric carcinoma (n=11), and ovarian cancer (n=10) were most frequently observed. Patient characteristics are summarized in the Table.

The highest cardiac signal intensities were measured 10 minutes after FAPI administration (median SUV, 1.39 [IQR, 0.62]). Signals decreased more rapidly within the first hour until a median SUV of 1.01 (IQR, 0.39) was measured. SUVs further decreased to median levels of 0.72 (IQR, 0.22) 3 hours after administration (Figure I in the [Data Supplement](#)). After 1 hour, the median blood pool SUV was 0.93 (IQR, 0.32). Signal intensity ratios between the heart and other organs differed greatly: heart/blood pool 0.93 (IQR, 0.38), heart/brain 12.44 (IQR, 13.29), heart/gluteal muscle 0.99 (IQR, 0.48), heart/liver 1.17 (IQR, 0.56), heart/lung 0.84 (IQR, 0.29). Twenty-one patients also had data from FDG-PET-CT scans. Left ventricular signal intensities were higher using an FDG tracer (Figure II in the [Data Supplement](#)). Comparing FDG and FAPI signals in each measured segment, we were able to see a relatively weak but consistent positive correlation ($r_s=0.36$, $P<0.0001$). Heart/blood and heart/lung signal ratios were comparable, heart/liver and heart/brain signal ratios were significantly higher in FAPI scans and, as FDG signals are indicative of glycolytic activity, heart/gluteus ratios were significantly higher in FDG scans.

Patients with prostate cancer and ovarian cancer showed nominally increased cardiac SUVs (1.08 [IQR, 0.63] and 1.04 [IQR, 1.84], respectively), whereas pancreatic cancer patients exhibited a nominal decrease (0.79 [IQR, 0.57]). Comparing solely these groups cardiac signals in patients with ovarian and prostatic cancer were significantly higher than in hearts from pancreatic cancer patients ($P=0.028$, Wilcoxon rank-sum test, Figures III and IV in the [Data Supplement](#)).

Table. Patient Characteristics

Patient Characteristics	Initial Cohort; N=185		Confirmatory Cohort N=44		Outliers N=11	
FAPI SUV Left Ventricle	0.98	(IQR: 0.55)	0.87	(IQR: 0.39)	2.97	(IQR: 0.66)
FAPI pattern left ventricle						
Focal	42		7		0	
Diffuse	61		21		4	
Homogen	82		16		7	
FAPI SUV aorta	1.14	(IQR, 0.47)	1.24	(IQR, 0.30)	1.61	(IQR, 0.53)
FAPI SUV brain	0.08	(IQR, 0.07)	0.07	(IQR, 0.06)	0.06	(IQR, 0.06)
FAPI SUV liver	0.86	(IQR, 0.5)	0.85	(IQR, 0.30)	1.44	(IQR, 0.73)
FAPI SUV gluteus	1.00	(IQR, 0.33)	1.02	(IQR, 0.30)	1.12	(IQR, 0.32)
Sex	Male: 119	Female: 66	Male: 30	Female: 14	Male: 7	Female: 4
Age, y	64	(IQR, 17)	65	(IQR, 20)	77	(IQR, 14)
BMI, kg/m ²	24.15	(IQR, 4.72)	25.82	(IQR, 4.79)	23.86	(IQR, 6.09)
TSH, mU/L	1.23	(IQR, 1.19)	1.08	(IQR, 0.92)	1.12	(IQR, 0.72)
Creatinine, μmol/L	65	(IQR 27)	71	(IQR, 33)	72	(IQR, 24)
Urea nitrogen, mmol/L	11.43	(IQR, 6.07)	11.43	(IQR, 4.82)	9.64	(IQR, 5.18)
C-reactive protein, mg/L	11	(IQR, 23)	29	(IQR, 37)	48	(IQR, 53)
Previous radiation to the chest	21	of 185	2	of 44	1	of 11
Coronary artery disease	27	of 185	4	of 44	4	of 11
Heart failure	2	of 185	0	of 44	0	of 11
Arterial hypertension	60	of 185	15	of 44	6	of 11
Atrial fibrillation	14	of 185	2	of 44	1	of 11
Diabetes mellitus type II	24	of 185	4	of 44	1	of 11
Active smoker	24	of 185	7	of 44	3	of 11
Cardiac medication						
ARB/ACE inhibitor	41	of 185	6	of 44	4	of 11
Beta-blocker	27	of 185	5	of 44	2	of 11
Statins	21	of 185	3	of 44	1	of 11
Daily aspirin	27	of 185	5	of 44	3	of 11
Cancer entities						
Pancreatic carcinoma	42	of 185	1	of 44	1	of 11
Bronchial carcinoma	20	of 185	3	of 44	1	of 11
Colorectal carcinoma	14	of 185	2	of 44	1	of 11
Oropharyngeal carcinoma	13	of 185	2	of 44	0	of 11
Esophageal/gastric carcinoma	11	of 185	2	of 44	0	of 11
Prostate carcinoma	11	of 185	3	of 44	2	of 11
Ovarian carcinoma	10	of 185	0	of 44	3	of 11
Other	64	of 185	31	of 44	3	of 11
Previous CTx						
Anthracyclines	28	of 185	4	of 44	5	of 11
Antibodies	26	of 185	2	of 44	1	of 11
Antimetabolites	92	of 185	8	of 44	5	of 11
Platinum derivatives	91	of 185	8	of 44	6	of 11
Alkylating agents	23	of 185	4	of 44	4	of 11
Topoisomerase inhibitors	39	of 185	0	of 44	1	of 11
Checkpoint inhibitors	21	of 185	2	of 44	1	of 11

ACE indicates angiotensin-converting enzyme; ARB, angiotensin-receptor-blocker; BMI, body mass index; CTx, chemotherapy; FAPI, fibroblast activation protein inhibitor; IQR, interquartile range; SUV, standardized uptake values; and TSH, thyroid-stimulating hormone.

Signal Intensity Correlates With Diabetes Mellitus, Different Chemotherapies, and Radiation to the Chest

In an univariate regression analysis, high left ventricular signals correlated with the presence of cardiovascular risk factors (OR, 4.3, $P=0.0029$), a focal myocardial signal pattern (OR, 3.9, $P=0.0068$), diabetes mellitus (OR, 4.1, $P=0.046$), and beta-blocker use (OR, 3.8, $P=0.049$).

Multivariate regression models were established following model optimization using Akaike information criterion. The models revealed a positive correlation of left ventricular signals with TSH levels above 4 $\mu\text{U/mL}$ (OR, 8.6, $P=0.012$), a body mass index above 25 kg/m^2 (OR, 2.6, $P=0.023$), previous radiation to the chest (OR, 3.5, $P=0.024$), previous intake of platinum derivatives (OR: 3.0, $P=0.034$), and a history of diabetes mellitus (OR, 2.9, $P=0.041$), whereas checkpoint inhibitor use was associated with a decreased signal intensity (OR, 0.17, $P=0.0496$; see Figure 1). A direct comparison comprising both cohorts and each subgroup is reported in Figure V in the [Data Supplement](#). Echocardiographic findings were available in a subgroup of patients ($n=44$). Increased FAPI signals were associated with reduced ejection fraction in a small number of patients (see Figure VI in the [Data Supplement](#)).

Multivariate Linear Prediction Model and Outlier Analysis Reveals Doxorubicin Therapy as a Potentially Relevant Variable in Cardiac FAP-Activity

To test for the reliability of our retrospective analysis, we further created a linear multivariate regression model based on the results of the logistic regression analyses. This model was used to find outliers in our dataset by selecting 5% of patients with the highest residuals (cutoff: 1.64). A permutation test with 100 000 permutations revealed that patients with ovarian and prostate cancer ($P=0.0056$) and patients receiving anthracyclines ($P=0.021$) or alkylating agents ($P=0.047$) were significantly overrepresented in our outlier cohort of patients with unexpectedly high cardiac FAPI signals.

We confirmed our prediction model in another cohort of 44 consecutive patients, which were scanned after our first cohort. In this confirmatory cohort, we were not able to find any outliers using the same metrics as we had in the first cohort (see Figure 1). There was no significant difference between the mean residuals of the 2 cohorts ($P=0.16$, Student t test). The SD was even slightly smaller in the confirmatory cohort. Patient characteristics of the confirmatory cohort are reported in Table.

Focal Signal Enrichment and Increased Signal Intensity Associated With Cardiovascular Risk and Disease

Signal patterns differed between the patients. Five distinct patterns were noted: homogenous, diffuse, focal on diffuse, focal, and weak enrichment. Significantly more patients with known cardiovascular risk factors exhibited a focal signal pattern ($P<0.0001$, Yate χ^2 -test). A focal myocardial enrichment pattern was negatively correlated with female sex (OR, 0.13, $P=0.0059$), whereas a positive correlation was seen for patients with hypertension (OR, 3.7, $P=0.0067$), known cardiac disease (OR, 3.8, $P=0.014$), known coronary heart disease (OR, 4.0, $P=0.029$), and medication with aspirin (OR, 4.8, $P=0.0069$) or statins (OR, 5.7, $P=0.0069$) in univariate logistic regression. In an optimized multivariate logistic regression model, only female sex (OR, 0.12, $P=0.0004$), known cardiovascular risk factors (OR, 5.1, $P=0.0008$), and aspirin use (OR, 3.0, $P=0.041$) were significantly associated (Figure 1).

Cardiac FAPI Signals Are Higher in Septal Segments and Slightly Increase Over Time

Analyzing FAPI signals in the 17-segment model of the left ventricle, we noticed a significantly higher signal in septal signals than in the lateral segments (septal versus lateral wall: $P=0.0038$; septal versus anterior/posterior wall: $P<0.0001$; lateral versus anterior/posterior wall $P=0.31$).

Considering all 17 segments, repetitive scans in 26 patients revealed an increase in FAP density over time in all segments ($P<0.0001$, Figure VII in the [Data Supplement](#)).

Interestingly, a series of patients with a history of myocardial infarction did not show increased signal intensities years following myocardial infarction (Figure VIII in the [Data Supplement](#)). Further investigation of all patients with known coronary artery disease showed that coronary artery disease does not correlate directly with FAPI intensities. One patient scanned while on radiotherapy in close proximity to the heart showed a striking increase in myocardial FAPI intensities (see Figure IX in the [Data Supplement](#)).

DISCUSSION

In this study, we report an association between fibroblast activation (FAP) density measured by FAPI-PET-CT scans and risk factors for cardiovascular disease in cancer patients. An increase in signal intensity was associated with hypothyroid metabolic state, overweight, and diabetes mellitus, suggesting an involvement of metabolic changes along with cardiac FAP activation. Fur-

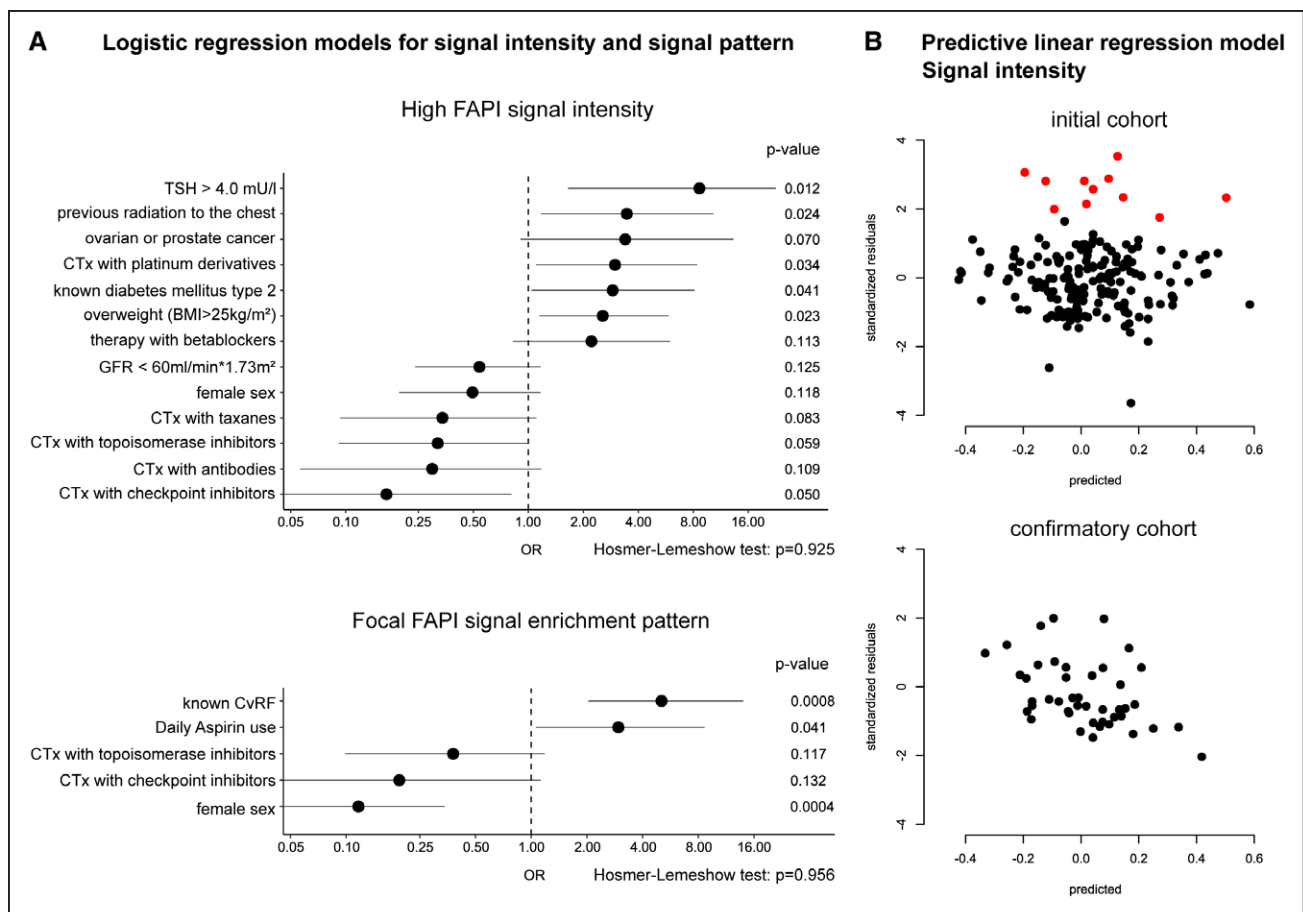


Figure 1. Logistic regression and linear prediction model for FAPI (fibroblast activation protein inhibitor) signal in the myocardium.

A, Multivariate logistic regression models for signal intensity and focal enrichment. Odds ratios (OR) are depicted as a dot. Lines mark the 95% CI. Although metabolic variables, such as increased thyroid-stimulating hormone (TSH), radiation, diabetes mellitus, overweight, and different chemotherapies, are associated with an increased FAPI signal, focal FAPI enrichment patterns are mainly associated with cardiovascular risk. N=185 for both analyses. **B**, Linear regression model for FAPI signal intensity prediction and outlier analysis based on significant variables of the multivariate logistic regression analysis. The model was established with the initial cohort (N=185) and tested for accuracy with a confirmatory cohort (N=44). Outliers (N=11) are marked in red in both plots. Outliers were defined as patients with residuals (actual–predicted FAPI signal) above the 95% mark of the initial cohort. Patient characteristics of the outlier cohort are reported in Table. BMI indicates body mass index; CTx, chemotherapy; CvRF, cardiovascular risk factors; and GFR, glomerular filtration rate.

thermore, radiation to the chest was associated with an increased cardiac FAPI signal. Focal enrichment patterns were associated with coronary artery disease, the presence of cardiovascular risk factors, and aspirin intake.

Local inflammatory response or intermittent local ischemia could be a possible explanation for this focal accumulation of FAPI signals. This notion is supported by preclinical data, where myocardial ischemia lead to an increase in FAP expression in affected segments.² Additionally, small-animal FAPI-PET-CT scans of the heart detected a sudden increase followed by a steady decline in FAP density following myocardial infarction.^{4,5} The peak in signal intensity only lasts a couple of days and marked the process of myocardial wound healing.^{2,4} We noted increased FAPI signals in close proximity to a cardiovascular event, whereas signals disappeared months to years after the event (Figures VIII and IX in the [Data Supplement](#)). This points towards a similar mechanism of FAP activation in the human heart. Mechanistically, inflammation is discussed as one cause of FAP activation.¹⁹ In line with this

interpretation, we detected a high cardiac FAPI signal in one patient scanned while receiving chest radiation, which is known to trigger a cardiac inflammatory response.

Aside from myocardial ischemia and inflammation, FAP-positive cells were recently identified to play a crucial role in catecholamine-induced cardiac remodeling and dysfunction. Accordingly, the elimination of FAP expressing cells led to a significant reduction in cardiac fibrosis and an increased systolic function in mice following administration of angiotensin II and phenylephrine.⁶ The development of excessive fibrosis and activation of fibroblasts are based on a direct crosstalk between fibroblasts and cardiomyocytes involving paracrine secretion of TGF β (transforming growth factor β). These processes seem to determine cardiac function and discriminate adaptive from maladaptive cardiac remodeling.^{20,21} Previous studies showed a suppressive effect of thyroid hormone on TGF β signaling, which possibly explains higher myocardial FAPI signal levels in hypothyroid patients in our study.²² Although aspirin is known to suppress TGF β

signaling, patients taking aspirin exhibited much higher cardiac FAPI signal intensities and were more likely to show focal enrichment patterns than patients not taking aspirin (see Figure 1 and Figure IV in the [Data Supplement](#)). The increase in fibroblast activation seen in this patient subgroup is most likely explained by other contributing factors, as aspirin use can be seen as a surrogate for an existing cardiovascular risk.²³

Interestingly, although a single cardiovascular risk factor led to a relatively mild increase in signal intensity, patients with multiple risk factors exhibited a more pronounced increase (Figure 2). FAPI signal enrichment was most noticeable in patients with arterial hypertension and metabolic diseases characterized by diabetes mellitus and obesity (Figure 2 and Figure IV in the [Data Supplement](#)). These findings are supported by animal data from diabetes mellitus models and transaortic constriction (artifi-

cial increase in afterload): both models promote cardiac hypertrophy and excessive cardiac fibrosis.^{24,25} Mechanistically, cardiac fibrosis in these models was caused by activated inflammatory pathways and TGFβ/Mothers Against Decapentaplegic Homolog Protein signaling. The increase in FAPI signaling in the human heart could, therefore, be a result of a concomitant dysregulation of metabolic and prohypertrophic pathways. Therefore, it will be important to link higher FAPI intensities to other cardiac imaging modalities (eg, cardiac MRI) to characterize cardiac tissue composition and function.

Study Limitations

Although recent data on FAP as well as our data on FAPI imaging provide important evidence for the use of FAPI-PET-CT scans to evaluate cardiac fibroblast activation,

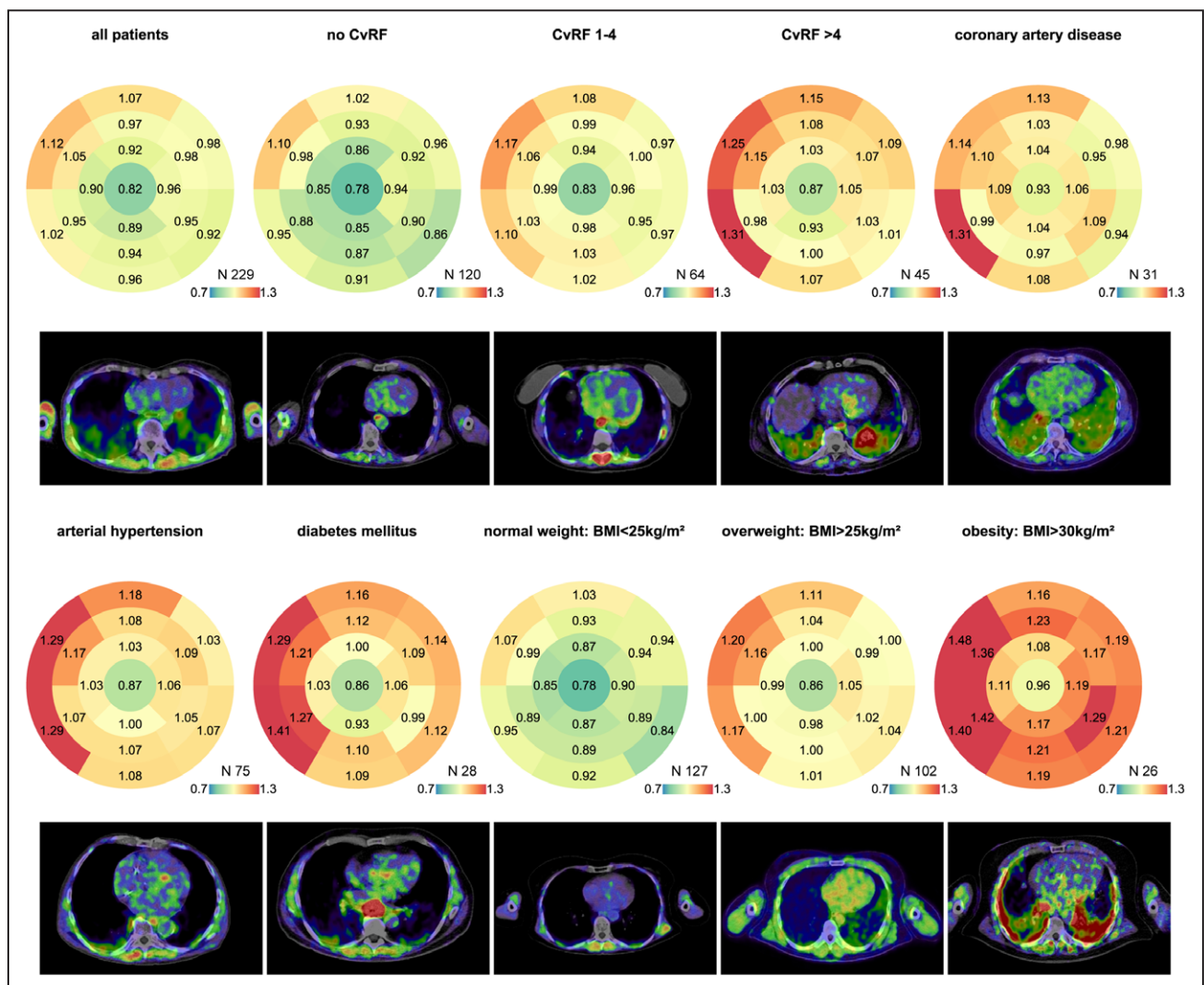


Figure 2. Bullseye 17-segment analysis of different subgroups with representative FAPI (fibroblast activation protein inhibitor) images. The median signal intensity of the corresponding segment is displayed for each group. The number of patients in a group is seen in the right lower corner of each bullseye above the color scale. The color coding was taken from a spectral color scale ranging from 0.7 (blue) to 1.3 (red) with 1.0 (yellow) being the center. Representative FAPI images are displayed below. Signal intensity was generally increased in the septal basal segments. The apex exhibited the lowest signal intensity. This effect was most pronounced in arterial hypertension. Diabetes mellitus, arterial hypertension, and obesity—all risk factors associated with metabolic stress and cardiac remodeling—show the highest increase in FAPI signals. BMI indicates body mass index; and CvRF, cardiovascular risk factors.

there are some limitations to our analysis. The analysis was retrospective and consisted mostly of single cross-sectional measurements in a heterogeneous patient cohort. In addition, only a minority of our scans were ECG-triggered, which might lead to an underestimation of signal intensities at the lateral wall and in the apex (Figure 2).

To account for bias in variable selection, we used Akaike information criterion to select the variables and used the Hosmer-Lemeshow goodness of fit test to assess the quality of our models. To further address potential biases based on a retrospective analysis,²⁶ we evaluated our model in another unselected cohort and retrieved similar results.

Although FAP is mainly expressed in granulation tissue, reactive stromal fibroblasts, and malignant cells, we cannot rule out that other cell types might contribute to the cardiac FAPI signal.²⁷ Inflammation induced FAP activation in cardiomyocytes, fibroblasts, or even endothelial cells (as seen in vascular disease), might be a contributing factor in some of our patients, especially since CRP (C-reactive protein) levels are increased in our outlier cohort (see Table).¹⁹

Conclusions

High FAPI signal intensities are associated with cardiovascular and metabolic risk factors, specifically arterial hypertension, diabetes mellitus, and obesity. Furthermore, a focal enrichment pattern could be suggestive of an underlying cardiovascular disease. Further research systematically comparing FAPI-PET-CT scans to other cardiac imaging modalities and possibly gene expression profiles will be necessary to open the route into clinical routine.

ARTICLE INFORMATION

Received February 19, 2020; accepted July 31, 2020.

This manuscript was sent to Victor G. Davila-Roman, MD, Executive Editor, for review by expert referees, editorial decision, and final disposition.

The Data Supplement is available at <https://www.ahajournals.org/doi/suppl/10.1161/CIRCIMAGING.120.010628>.

Correspondence

Lorenz Lehmann, MD, Cardio-Oncology Section, Department of Cardiology, Angiology, and Pneumology, Heidelberg University Hospital, INF 410, 69120 Heidelberg. Email lorenz.lehmann@med.uni-heidelberg.de

Affiliations

Department of Cardiology, Angiology, and Pneumology (M.B.H., F.R., D.F., H.A.K., F.L., L.H.L.) and Department of Nuclear Medicine (U.H.), Heidelberg University Hospital, Germany. German Centre for Cardiovascular Research (DZHK), Heidelberg/Mannheim partner site, Germany (M.B.H., F.R., D.F., H.A.K., F.L., L.H.L.). Clinical Cooperation Unit Nuclear Medicine, DKFZ, Heidelberg, Germany (U.H.). Translational Lung Research Center Heidelberg (TLRC), German Center for Lung Research (DZL), Heidelberg, Germany (U.H.). German Cancer Research Center (L.H.L.).

Acknowledgments

We thank Thomas Lindner, Christian Kleist, Susanne Krämer, Stephanie Biedenstein, Kirsten Kunze, and Anna Lesikov for excellent radiochemical and technical assistance.

Source of Funding

M.B. Heckmann is recipient of a fellowship of the DZHK (German Centre for Cardiovascular Research)

Disclosures

U. Haberkorn has a patent application for quinoline based FAP (fibroblast activation protein)-targeting agents for imaging and therapy in nuclear medicine and has shares of a consultancy-group for iTheragnostics. The authors filed a patent application for quinoline based FAP-targeting agents for the diagnosis of cardiovascular disease.

REFERENCES

1. Curley D, Lavin Plaza B, Shah AM, Botnar RM. Molecular imaging of cardiac remodelling after myocardial infarction. *Basic Res Cardiol*. 2018;113:10. doi: 10.1007/s00395-018-0668-z
2. Tillmanns J, Hoffmann D, Habbaba Y, Schmitto JD, Sedding D, Fraccarollo D, Galuppo P, Bauersachs J. Fibroblast activation protein alpha expression identifies activated fibroblasts after myocardial infarction. *J Mol Cell Cardiol*. 2015;87:194–203. doi: 10.1016/j.yjmcc.2015.08.016
3. Kaur H, Takefuji M, Ngai CY, Carvalho J, Bayer J, Wietelmann A, Poetsch A, Hoelper S, Conway SJ, Möllmann H, et al. Targeted ablation of periostin-expressing activated fibroblasts prevents adverse cardiac remodeling in mice. *Circ Res*. 2016;118:1906–1917. doi: 10.1161/CIRCRESAHA.116.308643
4. Varasteh Z, Mohanta S, Robu S, Braeuer M, Li Y, Omidvari N, Topping G, Sun T, Nekolla SG, Richter A, et al. Molecular imaging of fibroblast activity after myocardial infarction using a 68Ga-labeled fibroblast activation protein inhibitor, FAPI-04. *J Nucl Med*. 2019;60:1743–1749. doi: 10.2967/jnumed.119.226993
5. Nagaraju CK, Dries E, Popovic N, Singh AA, Haemers P, Roderick HL, Claus P, Sipido KR, Driesen RB. Global fibroblast activation throughout the left ventricle but localized fibrosis after myocardial infarction. *Sci Rep*. 2017;7:10801. doi: 10.1038/s41598-017-09790-1
6. Aghajanian H, Kimura T, Rurik JG, Hancock AS, Leibowitz MS, Li L, Scholler J, Monslow J, Lo A, Han W, et al. Targeting cardiac fibrosis with engineered T cells. *Nature*. 2019;573:430–433. doi: 10.1038/s41586-019-1546-z
7. Lindner T, Loktev A, Altmann A, Giesel F, Kratochwil C, Debus J, Jäger D, Mier W, Haberkorn U. Development of quinoline-based theranostic ligands for the targeting of fibroblast activation protein. *J Nucl Med*. 2018;59:1415–1422. doi: 10.2967/jnumed.118.210443
8. Giesel FL, Kratochwil C, Lindner T, Marschalek MM, Loktev A, Lehnert W, Debus J, Jäger D, Flechsig P, Altmann A, et al. 68Ga-FAPI PET/CT: biodistribution and preliminary dosimetry estimate of 2 DOTA-containing FAP-targeting agents in patients with various cancers. *J Nucl Med*. 2019;60:386–392. doi: 10.2967/jnumed.118.215913
9. Loktev A, Lindner T, Mier W, Debus J, Altmann A, Jäger D, Giesel F, Kratochwil C, Barthe P, Roumestand C, et al. A tumor-imaging method targeting cancer-associated fibroblasts. *J Nucl Med*. 2018;59:1423–1429. doi: 10.2967/jnumed.118.210435
10. Ortiz-Pérez JT, Rodríguez J, Meyers SN, Lee DC, Davidson C, Wu E. Correspondence between the 17-segment model and coronary arterial anatomy using contrast-enhanced cardiac magnetic resonance imaging. *JACC Cardiovasc Imaging*. 2008;1:282–293. doi: 10.1016/j.jcmg.2008.01.014
11. Cerqueira MD, Weissman NJ, Dilsizian V, Jacobs AK, Kaul S, Laskey WK, Pennell DJ, Rumberger JA, Ryan T, Verani MS; American Heart Association Writing Group on Myocardial Segmentation and Registration for Cardiac Imaging. Standardized myocardial segmentation and nomenclature for tomographic imaging of the heart. A statement for healthcare professionals from the Cardiac Imaging Committee of the Council on Clinical Cardiology of the American Heart Association. *Circulation*. 2002;105:539–542. doi: 10.1161/hc0402.102975
12. R Core Team. R. A Language and Environment for Statistical Computing. R Found Stat Comput 2018:Version: 3.6.2. <https://www.r-project.org/>. Accessed December 18, 2019
13. Neuwirth E. RColorBrewer: ColorBrewer Palettes. R Packag 2014:Version: 1.1-2. <https://cran.r-project.org/package=RColorBrewer>. Accessed December 18, 2019
14. Soetaert K. Shape: Functions for Plotting Graphical Shapes, Colors. R Packag 2018:Version: 1.4.4. <https://cran.r-project.org/package=Shape>. Accessed December 18, 2019
15. Heckmann MB, Totakhel B, Finke D, Anker MS, Müller-Tidow C, Haberkorn U, Katus HA, Lehmann LH. Evidence for a cardiac metabolic switch in

- patients with Hodgkin's lymphoma. *ESC Heart Fail*. 2019;6:824–829. doi: 10.1002/ehf2.12475
16. Venables WN, Ripley BD. *Modern Applied Statistics with S*. 4th ed. New York, NY: Springer; 2002.
 17. Wickham H. *ggplot2: Elegant Graphics for Data Analysis*. New York, NY: Springer-Verlag; 2009.
 18. Zhang Z. Variable selection with stepwise and best subset approaches. *Ann Transl Med*. 2016;4:136. doi: 10.21037/atm.2016.03.35
 19. Brokopp CE, Schoenauer R, Richards P, Bauer S, Lohmann C, Emmert MY, Weber B, Winnik S, Aikawa E, Graves K, et al. Fibroblast activation protein is induced by inflammation and degrades type I collagen in thin-cap fibroatheromata. *Eur Heart J*. 2011;32:2713–2722. doi: 10.1093/eurheartj/ehq519
 20. Kreusser MM, Lehmann LH, Keranov S, Hoting MO, Oehl U, Kohlhaas M, Reil JC, Neumann K, Schneider MD, Hill JA, et al. Cardiac CaM Kinase II genes δ and γ contribute to adverse remodeling but redundantly inhibit calcineurin-induced myocardial hypertrophy. *Circulation*. 2014;130:1262–1273. doi: 10.1161/CIRCULATIONAHA.114.006185
 21. Ottaviano FG, Yee KO. Communication signals between cardiac fibroblasts and cardiac myocytes. *J Cardiovasc Pharmacol*. 2011;57:513–521. doi: 10.1097/FJC.0b013e31821209ee
 22. Alonso-Merino E, Martin Orozco R, Ruiz-Llorente L, Martinez-Iglesias OA, Velasco-Martin JP, Montero-Pedrazuela A, Fanjul-Rodriguez L, Contreras-Jurado C, Regadera J, Aranda A. Thyroid hormones inhibit TGF-beta signaling and attenuate fibrotic responses. *Proc Natl Acad Sci USA*. 2016;113:E3451–E3460. doi: 10.1073/pnas.1506113113
 23. Stuntz M, Bernstein B. Recent trends in the prevalence of low-dose aspirin use for primary and secondary prevention of cardiovascular disease in the United States, 2012–2015. *Prev Med Reports*. 2017;5:183. doi: 10.1016/j.pmedr.2016.12.023
 24. Cavallera M, Wang J, Frangogiannis NG. Obesity, metabolic dysfunction, and cardiac fibrosis: pathophysiological pathways, molecular mechanisms, and therapeutic opportunities. *Transl Res*. 2014;164:323–335. doi: 10.1016/j.trsl.2014.05.001
 25. Müller OJ, Heckmann MB, Ding L, Rapti K, Rangrez AY, Gerken T, Christiansen N, Rennefahrt UEE, Witt H, González Maldonado S, et al. Comprehensive plasma and tissue profiling reveals systemic metabolic alterations in cardiac hypertrophy and failure. *Cardiovasc Res*. 2019;115:1296–1305. doi: 10.1093/cvr/cvy274
 26. Grouse L. Post hoc ergo propter hoc. *J Thorac Dis*. 2016;8:E511–E512. doi: 10.21037/jtd.2016.04.49
 27. Scanlan MJ, Raj BK, Calvo B, Garin-Chesa P, Sanz-Moncasi MP, Healey JH, Old LJ, Rettig WJ. Molecular cloning of fibroblast activation protein alpha, a member of the serine protease family selectively expressed in stromal fibroblasts of epithelial cancers. *Proc Natl Acad Sci USA*. 1994;91:5657–5661. doi: 10.1073/pnas.91.12.5657